Substrate-Integrated Coaxial Line Fed Air-Filled SIW Antenna for the 28 GHz 5G Bands

Laura Van Messem[1], Arno Moerman[2], Olivier Caytan[3], Hendrik Rogier[4], Sam Lemey[5]
IDLab-Electromagnetics group, imec-Ghent University, Belgium
{[1]laura.vanmessem, [2]arno.moerman, [3]olivier.caytan, [4]hendrik.rogier, [5]sam.lemey}@ugent.be

Abstract— **A compact, cost-effective antenna element for beamsteering applications is developed for efficient operation in the fifth-generation (5G) n257 (26.5 GHz, 29.5 GHz) and n261 (27.5 GHz, 28.35 GHz) frequency bands. An air-filled cavity-backed patch antenna topology is proposed. Feeding the antenna with a substrate-integrated coaxial line (SICL) feed yields excellent antenna-to-platform isolation, which is represented by a front-to-back ratio (FTBR) of at least 22 dB, while avoiding distortions in the radiation pattern. Moreover, this feed implementation allows rotation over 360° without any loss in performance. The total efficiency is increased (above 92%) by employing an air-cavity, resulting in an improved realized gain response, ranging from 7.25 dBi to 8.35 dBi, and a half-power beamwidth around 72°. By assembling single-layer standard manufactured printed circuit boards (PCBs), a cost-effective design is obtained.**

Keywords— **Air-filled substrate-integrated waveguide (AFSIW), antenna element, fifth-generation (5G) wireless communication, millimeterwave (mmWave), packaged, standard printed circuit board (PCB).**

I. Introduction

The proliferation of 5G technology and the increase in application areas has encouraged the transformation of our wireless networks towards joint communication and sensing (JCAS). Operating within the millimeterwave (mmWave) spectrum, the n257 (26.5 - 29.5 GHz) and the n261 (27.5 - 28.35 GHz) frequency bands are ideal for short range communications employing high datarates and for sensing applications achieving higher resolutions. The greater network capacity based on dense frequency reuse allows smaller communication cells, and even cell-free massive multiple-input multiple-output (mMIMO) [1]. However, the shift to higher frequencies inherently increases path loss. This can be mitigated by leveraging a greater number of antennas, effectively enlarging the radiating aperture. The increase in broadside gain comes at the cost of a narrower pencil beam radiation pattern, increasing the risk for beam misalignment. The development of highly efficient and compact antenna arrays capable of beamsteering emerge as a critical point. Beamsteering arrays enable controlling the direction of signal propagation, facilitating user-targeting.

The inter-antenna coupling of the elements can be improved by introducing a cavity into the antenna topology. Dielectric cavities are easily introduced in multi-layer topologies [2], [3], minimizing the required space for a full front-end implementation at the cost of increased dielectric loss. Cavity-backed air-filled topologies suppress this dielectric loss [4]. Additionally, they can be implemented by employing several single-layer printed circuit boards (PCBs), obtaining a cost-effective design [5], [6]. Substrate-integrated waveguide (SIW) is a popular feeding technique for these air-filled cavities, but becomes problematic when routing signals to large antenna arrays, whereas a more compact microstrip line feed causes significant back radiation and crosstalk. To this end, substrate-integrated coaxial line (SICL) technology combines the compactness and easy integration possibilities of grounded co-planar waveguide (GCPW) lines with the good power handling and self-shielding capabilities of SIW [7]. It has been used for packaged passive component implementations, such as filters [8] and couplers [9] among others. In summary, these advantages can be exploited to implement compact routing networks for antenna arrays [10], minimizing the inter-antenna element spacing to avoid grating lobes in the scan range.

In this paper, we focus on developing a highly-efficient air-filled cavity-backed patch antenna with excellent antenna-to-platform isolation using a PCB implementation. This performance is achieved by leveraging self-isolating signal distribution options, such as SICL routing and coax-like via transitions towards GCPW lines for interfacing with integrated circuits (ICs). A cost-effective design is obtained by employing multiple single-layer PCBs, fabricated in standard PCB manufacturing technology.

The proposed design is described in Section II, while the simulations and measurements are compared in Section III. In Section IV, the conclusion summarizes all figures of merit and outlines the advantages of this topology.

II. Antenna Design

The proposed SICL-fed air-filled cavity-backed patch antenna topology is depicted in Fig. 1. The indicated dimensions in millimeter are obtained after optimization for in-band return loss and radiation efficiency employing CST Microwave Studio's frequency solver. A GCPW line transitions to a SICL feed by means of a coax-like via transition. Thereafter, the signal is transferred trough an hourglass-shaped slot into the air-filled cavity, before exciting the radiating patch.

Five separate single-layered PCBs are used to implement the topology. Three 0.254 mm-thick RO4350B laminates with patterned 35 μm-thick conductor layers at both sides, including an electroless nickel immersion gold (ENIG) surface finish, are followed by a 1.0 mm-thick FR4 substrate with 35 μm-thick conductor layers at both sides to implement a milled and edge-plated air-filled cavity. The final 0.254 mm-thick RO4350B laminate includes only a single 35 μm-thick conductor to implement the radiating patch. The individual layers are assembled by securing nuts and bolts through the drilled alignment holes in each PCB layer, as demonstrated by the top view in Fig. 1.

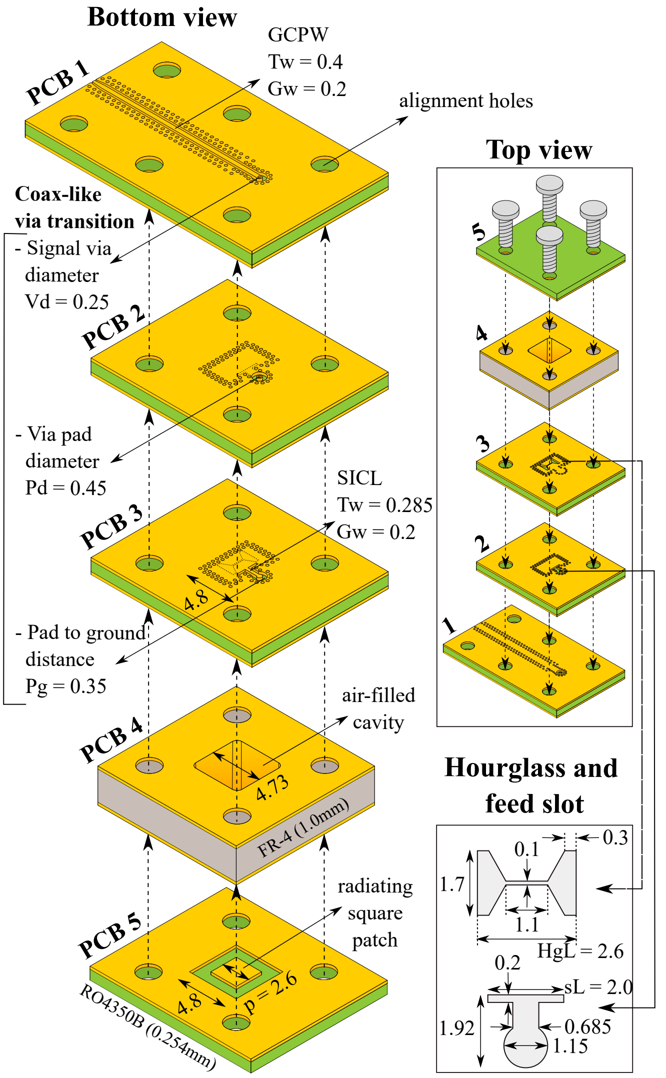

Fig. 1. Design of the proposed SICL antenna element with dimensions in millimeter, employing five separate standard PCBs.

The first PCB (PCB 1) implements a GCPW line, required for measurement purposes. In a next stage, this line can be routed towards a beamforming IC. At the end of this GCPW line, a coax-like via transition distributes the signal to a lower layer. It consists of a single signal via with diameter Vd=0.25 mm, surrounded by a dielectric mantel. The signal is contained by a circle of grounding vias of diameter Vd=0.25 mm at a distance of Ve=0.15 mm from the copper edge and with a center-to-center spacing of Vs=0.5 mm to suppress field-leakage.

The second PCB (PCB 2) serves as isolation layer between the GCPW line on PCB 1 and the SICL feed on the third PCB (PCB 3). The proposed coax-like transition, the GCPW line and the SICL feed are all matched to 50 Ω for optimal power transfer. Moreover, by separating them using a ground plane provided by PCB 2, we create an additional degree of rotational freedom: the GCPW and SICL can be oriented under any angle with respect to each other. This facilitates easy routing towards ICs. The dimensions of the feed slot on the conductor layer of PCB 2, at the side of PCB 3, are indicated at the bottom right in Fig. 1.

An hourglass-shaped coupling slot is etched on the third PCB (PCB 3), at the side of PCB 4, to provide coupling from the dielectric cavity excited by the SICL feed into the air-filled cavity. The hourglass shape is selected as resonant structure for broadband power transfer towards the air-filled cavity and provides a first resonant frequency of this design. The center of the hourglass slot is at 0.95 mm from the shorted end of the SICL feed. The boundaries of the dielectric cavity of PCB 3, including the SICL feed, fits within a footprint of 4.8 mm by 4.8 mm, which corresponds to $0.472\lambda_{0,29.5GHz} \times 0.472\lambda_{0,29.5GHz}$ when expressed in terms of free space wavelength at the highest operating frequency. Consequently, this grants a minimal inter-element spacing smaller than $0.5\lambda_{0,29.5GHz} \times 0.5\lambda_{0,29.5GHz}$ in a square lattice, mitigating any undesired grating lobes or blind spots when looking at array implementations.

The air-filled cavity in the fourth PCB (PCB 4) is implemented on a low-cost FR4 laminate by milling and edge-plating. The dimensions and the height of this cavity determine the coupling strength of the hourglass-shaped coupling slot towards the radiating patch, while mitigating any undesired inter-element coupling. The height of the cavity should be considered carefully, since a higher cavity increases the directivity, and consequently the broadside gain, at the cost of broadband matching. A cavity height of 1 mm for operating frequencies around 28 GHz results in a good trade-off between high-performance and achievable frequency range of operation.

The final PCB (PCB 5) is a 0.254 mm-thick RO4350B laminate with a single 35 μm-thick conductor on the bottom, at the side of PCB 4. The radiating patch is responsible for tuning the second resonance of this design. The footprint of the functional part of PCB 5 also remains smaller than $0.5\lambda_{0,29.5GHz} \times 0.5\lambda_{0,29.5GHz}$, allowing a maximal grating-lobe-free scan range. The proposed GCPW-to-SICL fed cavity-backed patch antenna is well-suited for efficient beamsteering array implementations.

III. Results

The fabricated PCB layers are assembled into a prototype, as shown in Fig. 2. The assembly is done by adding solder to the signal via pad on both sides of PCB 2. Thereafter, the assembled stack of five separate PCBs, including the nuts and bolts for alignation, is reflow soldered. Solder will thinly distribute over the available space, including part of the GCPW line, to provide the galvanic contact required for signal propagation through the coax-like via transition from GCPW to SICL.

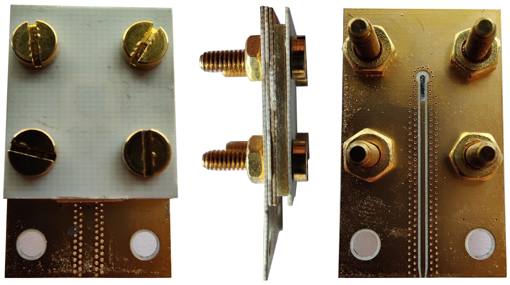

Fig. 2. Assembled prototype of the proposed SICL antenna element.

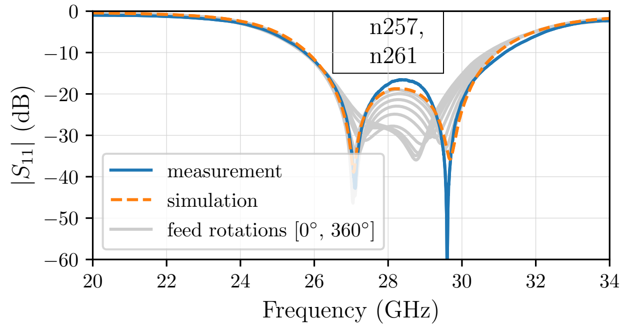

Fig. 4. The reflection coefficient of the proposed SICL antenna element.

The measurements of the prototype are performed with a Keysight N5247B PNA-X vector network analyzer (VNA), using solder-free SouthWest female 2.4 mm End Launch press-fit connectors. The measured scattering parameters (solid) are compared to the simulated S-parameters (dashed) in Fig. 4. The simulated reflection coefficient remains below −18 dB over the entire n257 and n261 frequency bands, while including a margin of 700 MHz on the upper side against manufacturing tolerances. The resonant patch dimensions (p) on PCB 5 determine the operating frequency. The resonance at the lowest frequency can be tweaked by altering the length of the hourglass-shaped slot (HgL) on PCB 3 and the second resonance is adjustable by changing the length of the feed slot (sL) on PCB 2 and PCB 3. This operating principle is clarified in Fig. 3.

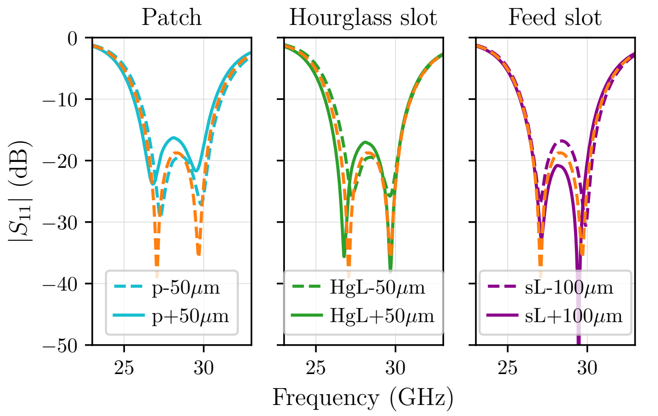

Fig. 3. The effect on the reflection coefficient of the proposed SICL antenna element for changing (left) patch dimensions (p), (middle) hourglass slot length (HgL), and (right) feed slot length (sL). The simulated nominal curve is represented by the orange dashed line.

The measured prototype shows excellent agreement with the simulations. The measured return loss across the envisaged frequency band of operation is better than 16.5 dB. Moreover, robust performance is demonstrated against rotations of the GCPW feed around the coax-like via transition, as shown in Fig. 4.

An anechoic chamber with an NSI-MI spherical antenna measurement system and a Keysight N5242A PNA-X VNA were used to measure the far-field radiation patterns through gain comparison with a WR-34 standard gain horn. The resulting measured (solid) and simulated (dashed) co-polarized radiation patterns at 26.5 GHz, 28 GHz and 29.5 GHz are shown in Fig. 5. The measured cross-polarized radiation pattern is represented by a dotted line. It remains more than 20 dB below the co-polarization component within the half-power beamwidth. The measured 3 dB beamwidth is 82°, 74°, 62° at 26.5 GHz, 28 GHz and 29.5 GHz, respectively. The broadside realized gain remains larger than 3 dBi from −40° to 40° within the n257 and n261 frequency bands.

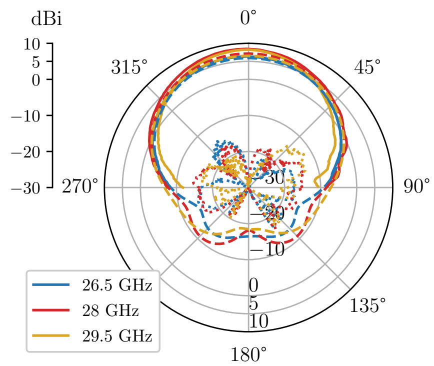

Fig. 5. Measured (solid) and simulated (dashed) realized gain co-polarization and the measured cross-polarized (dotted) radiation pattern of the proposed SICL antenna element.

The maximum realized gain as a function of frequency is shown in Fig. 6. The measured (simulated) values at 26.5 GHz, 28 GHz and 29.5 GHz are 7.2 dBi (7.0 dBi), 8.3 dBi (7.5 dBi) and 8.0 dBi (7.5 dBi), respectively. The measured maximum realized gain varies over 7.8±0.55 dBi in the n257 frequency band, representing a flat gain response. In the envisaged n257 and n261 frequency bands, the corresponding radiation efficiency remains above 93%, while the total efficiency is above 92%. A comparison of our proposed solution to other state-of-the-art antenna elements operating around 28 GHz can be found in Table 1.

IV. Conclusion

In this paper, we proposed a substrate-integrated coaxial line (SICL) fed air-filled cavity-backed patch antenna to obtain a highly-efficient element with excellent antenna-to-platform isolation. The element fits within a footprint of $0.48\lambda_{0,29.5GHz} \times 0.48\lambda_{0,29.5GHz}$ with a

Table 1. Comparison of antenna elements operating around 28 GHz.

Ref.	Element Max. Gain (dBi)	Radiation Efficiency (%)	Size (mm x mm)
[11]	6.9	87.1	33 x 27.5
[12]	4.95	83	5.3 x 5.3
[13]	4.71	88.8	26 x 26
[14]	8.1	92.5	5.5 x 5.5
[15]	7.4	90	4.6 x 4.6
This work	8.35	93	4.8 x 4.8

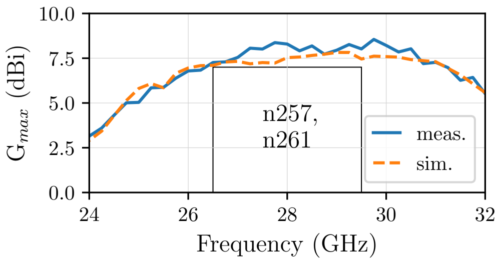

Fig. 6. Measured maximum (broadside) realized gain of the proposed SICL antenna element.

good inter-element isolation by employing an edge-plated cavity, rendering it suitable for advanced beamsteering applications. The measured maximum realized gain varies within 7.8±0.6 dBi over the envisaged n257 (26.5 GHz, 29.5 GHz) and n261 (27.5 GHz, 28.35 GHz) frequency bands. Moreover, the proposed design allows trading in performance in terms of matching and realized gain to obtain more bandwidth, covering all global 28 GHz 5G bands, including the n258 band (24.25 GHz, 27.5 GHz). The rotational freedom of the grounded co-planar waveguide (GCPW) feed over 360°, owing to the coax-like via transition, eases integration challenges with active electronics. The integrated circuits (ICs) can be integrated on the back of the printed circuit board (PCB) stack owing to the excellent antenna-to-platform isolation. Direct interfacing with compact GCPW lines minimizes interconnect losses in future adaptive beamforming multi-antenna systems for next-generation wireless communication and sensing applications. During the conference, a completely packaged beamsteering antenna array will be shown.

REFERENCES

[1] A. Moerman, J. Van Kerrebrouck, O. Caytan, *et al.*, "Beyond 5G without obstacles: mmWave-over-fiber distributed antenna systems," *IEEE Communications Magazine*, vol. 60, no. 1, pp. 27–33, 2022.

[2] H. R. D. Filgueiras and A. C. Sodré, "A 64-element and dual-polarized SICL-based slot antenna array development applied to TDD massive MIMO," *IEEE Antennas and Wireless Propagation Letters*, vol. 21, no. 4, pp. 750–754, 2022.

[3] N. Baghel and S. Mukherjee, "A Novel Half Mode SICL Based Dual Beam Antenna Array for Ka-band Application," *IEEE Access*, 2023.

[4] C. Dong, Y. You, S. Shen, *et al.*, "Dual Circularly-Polarized Septum Antenna Array Based on an Air-Filled Dual-Mode Feeding Network," *IEEE Transactions on Antennas and Propagation*, 2024.

[5] L. Van Messem, A. Moerman, O. Caytan, *et al.*, "A 4× 4 millimeterwave-frequency Butler matrix in grounded co-planar waveguide technology for compact integration with 5G antenna arrays," *IEEE Transactions on Microwave Theory and Techniques*, vol. 71, no. 1, pp. 122–134, 2022.

[6] I. L. de Paula, S. Lemey, D. Bosman, *et al.*, "Cost-effective high-performance air-filled SIW antenna array for the global 5G 26 GHz and 28 GHz bands," *IEEE Antennas and Wireless Propagation Letters*, vol. 20, no. 2, pp. 194–198, 2020.

[7] K. Wu, M. Bozzi, and N. J. Fonseca, "Substrate integrated transmission lines: Review and applications," *IEEE Journal of Microwaves*, vol. 1, no. 1, pp. 345–363, 2021.

[8] M. Cariou, B. Potelon, C. Quendo, *et al.*, "Compact X-Band Filter Based on Substrate Integrated Coaxial Line Stubs Using Advanced Multilayer PCB Technology," *IEEE Transactions on Microwave Theory and Techniques*, vol. 65, no. 2, pp. 496–503, 2016.

[9] L. Van Messem, A. Moerman, O. Caytan, H. Rogier, and S. Lemey, "Substrate Integrated Coaxial Line Millimeterwave Components Manufactured in Standard PCB," in *2023 IEEE 32nd Conference on Electrical Performance of Electronic Packaging and Systems (EPEPS)*, IEEE, 2023, pp. 1–3.

[10] F.-F. Fan, Q.-L. Chen, Y.-X. Xu, X.-F. Zhao, J.-C. Feng, and Z.-H. Yan, "A wideband compact printed dipole antenna array with SICL feeding network for 5G application," *IEEE Antennas and Wireless Propagation Letters*, vol. 22, no. 2, pp. 283–287, 2022.

[11] M. Usman, E. Kobal, J. Nasir, Y. Zhu, C. Yu, and A. Zhu, "Compact SIW fed dual-port single element annular slot MIMO antenna for 5G mmWave applications," *IEEE Access*, vol. 9, pp. 91 995–92 002, 2021.

[12] S. Tang, C.-Y. Chiu, and R. Murch, "A millimeter-wave tri-modal patch antenna," *IEEE Antennas and Wireless Propagation Letters*, vol. 21, no. 2, pp. 406–410, 2021.

[13] E. Kobal, R.-J. Liu, C. Yu, and A. Zhu, "A high isolation, low-profile, triple-port SIW based annular slot antenna for millimeter-wave 5G MIMO applications," *IEEE Access*, vol. 10, pp. 89 458–89 464, 2022.

[14] J.-E. Zhang, Q.-F. Zhang, W. Qin, W.-W. Yang, and J.-X. Chen, "Compact and Broadband Substrate Integrated Dielectric Resonator Antenna Suitable for 5G Millimeter-Wave Communications," *IEEE Open Journal of Antennas and Propagation*, 2023.

[15] J. Kowalewski, J. Eisenbeis, A. Jauch, J. Mayer, M. Kretschmann, and T. Zwick, "A mmW broadband dual-polarized dielectric resonator antenna based on hybrid modes," *IEEE Antennas and Wireless Propagation Letters*, vol. 19, no. 7, pp. 1068–1072, 2020.